Structural, electrical, and magnetic properties of $BaCo_{1-x}Cu_xS_2$

J. W. Schweitzer*
Department of Physics and Astronomy, University of Iowa, Iowa City, Iowa 52242, USA
(Received 5 January 2006; published 20 March 2006)

Compounds of the layered transition-metal-sulfide series $BaCo_{1-x}Cu_xS_2$ $(0 \leqslant x \leqslant 0.5)$ were prepared, and structural, electrical, and magnetic properties were investigated. The semiconductor $BaCoS_2$ is antiferromagnetically ordered below 310 K. With increasing Cu content x the structure becomes more anisotropic as the lattice parameter perpendicular to the layers elongates while the parallel parameter contracts. The resistivity is nonmetallic for all the compounds in this series. The Néel temperature T_N decreases with x, reaching $T_N \approx 0$ by $x \approx 0.2$. The susceptibility in the high-temperature paramagnetic phase, which for $BaCoS_2$ is consistent with Co^{2+} ions in the low-spin $S=1/2$ state, shows a Curie constant that is very much smaller than expected for Cu^{1+} and a mixture of Co^{2+} and Co^{3+} in the ratio of $1-2x$ to x. At sufficiently low temperatures there is a spin-glass phase for all $x>0$. The magnetic phase diagram obtained is remarkably similar to that of normal state $La_{2-x}Sr_xCuO_4$ $(x \leqslant 0.06)$.

DOI: 10.1103/PhysRevB.73.104426 PACS number(s): 75.30.Kz, 72.80.Ga, 75.50.Lk, 75.30.Mb

I. INTRODUCTION

Initial interest in $BaCoS_2$ was owing to the observation[1,2] that it is a layered Mott-Hubbard insulator that orders antiferromagnetically and therefore might be a sulfide analog to La_2CuO_4, the parent compound of the high-T_C cuprate superconductors. Unfortunately it has not been possible to create a superconducting phase by doping as in the case with $La_{2-x}(Ca,Sr,Ba)_xCuO_4$. However, by chemical substitution in $BaCoS_2$ it is possible to produce a rich diversity of structural, electronic, and magnetic phases as a function of temperature and chemical composition.

Substitution of Co by Ni produces a continuous change from the antiferromagnetic semiconducting phase to a paramagnetic metallic phase with the crossover in both the electrical and magnetic properties occurring near $x=0.25$ in the $BaCo_{1-x}Ni_xS_2$ $(0 \leqslant x \leqslant 1)$ series.[3–8] The sulfur-deficient $BaCo_{1-x}Ni_xS_{2-y}$ $(0.05 \leqslant x,y \leqslant 0.20)$ series[3,9] exhibits an unusual first-order transition from an antiferromagnetic insulator to a paramagnetic metal with decreasing temperature near 200 K that is associated with a major crystalline distortion to a structure of lower symmetry.[10]

It is also possible to replace up to 50% of the Co in $BaCoS_2$ with Cu. An earlier study[11] of the $BaCo_{1-x}Cu_xS_2$ found these compounds to be semiconductors with antiferromagnetic and spin-glass phases. Since Cu is always monovalent in sulfides, it is somewhat surprising that Cu can be substituted at finite concentrations and that the compounds do not become metallic with increasing Cu content. This study also investigated the nonstoichiometric $BaCo_{1-x}Cu_xS_{2-x/2}$ $(0 \leqslant x \leqslant 0.5)$ series where the Co, Cu, and S can have their normal valences. As expected for that series, the main effect of substituting diamagnetic $d^{10}Cu^{1+}$ for d^7Co^{2+} is the suppression of antiferromagnetic ordering of the d^7Co^{2+} spins.

In this paper a more thorough study of the $BaCo_{1-x}Cu_xS_2$ $(0 \leqslant x \leqslant 0.5)$ series is presented where the magnetic phases are characterized by both dc and ac magnetization measurements on a large number of samples. In the stoichiometric series the Cu substitution is expected to be a hole doping. Therefore, to the degree that $BaCoS_2$ is analogous to La_2CuO_4, the $BaCo_{1-x}Cu_xS_2$ system might be expected to be similar to the $La_{2-x}Sr_xCuO_4$ system. The results show that the rich variety of magnetic behaviors found in the normal state $La_{2-x}Sr_xCuO_4$ $(x \leqslant 0.06)$ are also exhibited by $BaCo_{1-x}Cu_xS_2$ $(0 \leqslant x \leqslant 0.5)$.

II. EXPERIMENTAL PROCEDURES

A. Synthesis

For this study single-phase polycrystalline samples of $BaCo_{1-x}Cu_xS_2$ $(0 \leqslant x \leqslant 0.5)$ were prepared using conventional solid-state reaction techniques starting with powders of the binary sulfides BaS, CoS (mixture of Co_9S_8 and hexagonal $CoS_{1.1}$), and CuS. Stoichiometric quantities of the reactants were mixed, pressed into pellets, and sealed in quartz tubing at a pressure less than 10 Torr. The sealed tubes were heated to 300 °C at 5 °C/min and held for 5 h, raised to a maximum reaction temperature T_{max} at 10 °C/min and held for 24–48 h, and quenched by dropping the tube into a water bath. The samples were then ground, pressed, resealed, and heated rapidly to T_{max} where the samples were held for 24–48 h before being quenched. The reaction temperature T_{max} was chosen by trial and error to be as close to the melting temperature as possible without causing plating of material on the wall of the quartz tube. The value of T_{max} decreased uniformly with Cu content from $T_{max} \approx 950$ °C at $x=0$ to $T_{max} \approx 650$ °C at $x=0.5$.

At most compositions several samples were produced from independent preparations that used differently prepared starting sulfides and/or slightly different reaction temperatures. $BaCoS_2$ is a metastable compound that must be prepared above 850 °C and rapidly quenched to prevent decomposition into Ba_2CoS_3 and CoS upon cooling. Although alloys with $x \geqslant 0.15$ appear stable, all samples were quenched for consistency. This method of synthesis yielded sintered, black, polycrystalline, single-phase samples for x

$\leqslant 0.5$, but failed to produce single-phase samples at higher Cu concentrations. The ferromagnetic compound CoS_2 ($T_C = 120$) was identified as a contaminant in preparations with $x \geqslant 0.5$.

B. Experimental details

Powder x-ray diffraction (XRD) patterns were obtained for all the samples at room temperature with a Siemens D 5000 diffractometer. The powder patterns were used to confirm the lattice structure, inspect for additional phases, and determine lattice constants. Resistance measurements as a function of temperature were made on bars cleaved from the sintered polycrystalline pellets. These measurements were performed with a current of 1 mA using a standard four-wire configuration with copper wire contacts that were attached to the samples with silver epoxy. The current was reversed during each measurement. For the characterization of the magnetic properties of the materials, dc and ac magnetization measurements were made using a Quantum Design superconducting quantum interference device (SQUID) magnetometer.

III. EXPERIMENTAL RESULTS

A. Crystal structure

The powder XRD patterns of the $BaCo_{1-x}Cu_xS_2$ compounds with $0.1 \leqslant x \leqslant 0.5$ are consistent with single-phase materials where the crystal structure is isostructural with $BaNiS_2$. The layered compound $BaNiS_2$ has a tetragonal structure with two formula units per unit cell and $P4/nmm$ symmetry.[12] The dimension of this tetragonal cell perpendicular to the layers is approximately twice the parallel dimension. In this structure Ni sites are pentacoordinated to S sites in a square-pyramidal environment. These edge-sharing pyramids alternate above and below the basal plane of sulfurs. The Ni atoms and these S atoms form $(NiS_{4/4})_2$ sheets within which the Ni atoms are displaced above and below the plane. The apical S atoms together with the Ba atoms form slightly distorted rock salt layers between these Ni-S sheets. The $BaCoS_2$ structure[2,13] is distinguished from the $BaNiS_2$ structure by a slight monoclinic distortion where the angle between the axes of the formerly square lattice of the layers opens from 90° to 90.45(2)° while leaving the two axes with equal lengths, and thus equivalently described by a twice as large C-centered orthorhombic unit cell. The observed rapid suppression of this monoclinic distortion with the substitution of Cu for Co agrees with the previous study[11] of this system and is also very similar to the stabilization of the tetragonal phase when Ni is substituted for Co as shown in studies[8] of the $BaCo_{1-x}Ni_xS_2$ series.

The lattice constants of the $BaCo_{1-x}Cu_xS_2$ unit cell determined from the powder patterns are shown in Fig. 1. For $x \geqslant 0.1$ the reflections were indexed using the tetragonal $BaNiS_2$ cell. The lattice constant a, which is the dimension in the plane parallel to the $(Co_{1-x}Cu_xS_{4/4})_2$ sheets, decreases with increasing Cu content x, while the perpendicular lattice constant c increases with x. The net effect of the substitution of Cu for Co is greater anisotropy for this layered compound

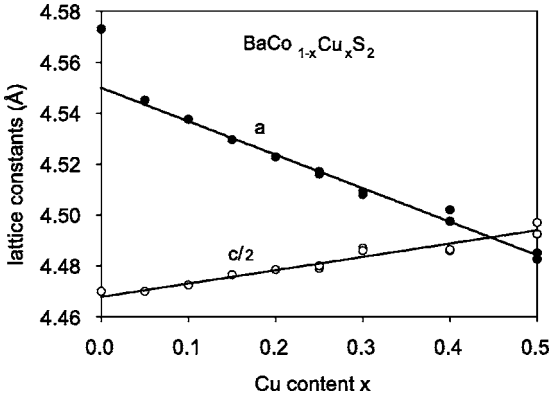

FIG. 1. Lattice constants parallel (a) and perpendicular (c) to the layers vs Cu content x at room temperature.

and a decrease in the volume of the cell. The point plotted at $x=0$ is the a lattice constant of the monoclinic $BaCoS_2$ cell, however, the monoclinic distortion is so small that the lattice constant is essentially the same as that for a tetragonal cell having the same volume. The linear variation of the lattice constants with x in the tetragonal phase ($x \geqslant 0.1$) suggests that the lattice deformation is confined to the site of substitution. The lines are linear fits to the lattice constants for $x \geqslant 0.1$. The extrapolation of the tetragonal phase data to $x=0$ yields a value for a that is 0.5% smaller than the actual value. There is clearly a significant contraction of the dimension parallel to the sheets accompanying the transition from the monoclinic to the tetragonal structure. Results are given for two independently prepared samples at each composition $x \geqslant 0.25$. The lack of agreement between the different samples at $x=0.4$ and 0.5 is much greater than the uncertainty in the lattice constants and is indicative of the difficulty of preparing stoichiometric compounds with the exact target composition. As x increases the materials produced are more likely to be suffer deficient and/or contain multiple phases. There are correlations with the starting sulfides and the reaction temperatures used in the synthesis.

B. Resistivity

Electrical resistivities for $BaCo_{1-x}Cu_xS_2$ were estimated from resistance measurements made on sintered polycrystalline bars taking into account only the geometric factors. Although the resistivities reported could differ significantly from the intrinsic resistivities owing to the granularity of the bars, the variation with Cu composition should be meaningful since the porosity and grain size appear similar in all the bars. The resistivities of these compounds all increase with decreasing temperature as can be seen in Fig. 2 where the resistivity is plotted as a function of $1/T$ for temperatures $T > 50$ K on a logarithmic scale. The total variation with temperature is greatest for $BaCoS_2$ and least for the $x=0.2$ compound. At the highest temperatures, the temperature dependence appears to be approaching an exponential behavior $\rho(T) \propto \exp(E_a/kT)$ where the activation energy E_a decreases rapidly with Cu composition from 0.15 eV at $x=0$ to 0.005 eV at $x=0.2$ and then increases to a value at $x=0.3$ which is approximately the same as that at $x=0.1$.

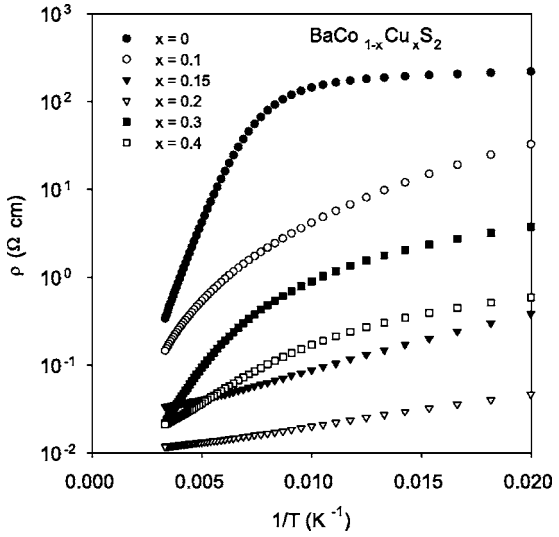

FIG. 2. Resistivity as a function of inverse temperature for temperatures above 50 K.

C. dc magnetic susceptibility

$BaCoS_2$ exhibits antiferromagnetic ordering with the Néel temperature T_N near 310 K. The magnetic structure has been reported based on neutron powder diffraction studies.[6,14,15] Within the $(CoS_{4/4})_2$ sheets the moments of adjacent Co atoms that lie above the basal plane of sulfurs are antiparallel, and similarly for the moments of the of the Co lying below. The magnetic unit cell is the same as the orthorhombic chemical cell with four formula units. The Co moments are colinear and confined to planes parallel to Co-S layers. In the dc magnetic susceptibility there is a broad asymmetric peak associated with this antiferromagnetic transition.

The temperature dependence of the magnetic susceptibility of $BaCo_{1-x}Cu_xS_2$, obtained from measurements of the magnetization as samples were cooled in a 5 kOe field, is shown in Fig. 3 for several samples in the composition range $x \leqslant 0.2$. The broad asymmetric peak associated with the antiferromagnetic transition in these layered compounds shifts rapidly to lower temperatures as the Cu concentration x increases. These measurements indicate that long-range antiferromagnetic ordering does not exist above $x \approx 0.2$.

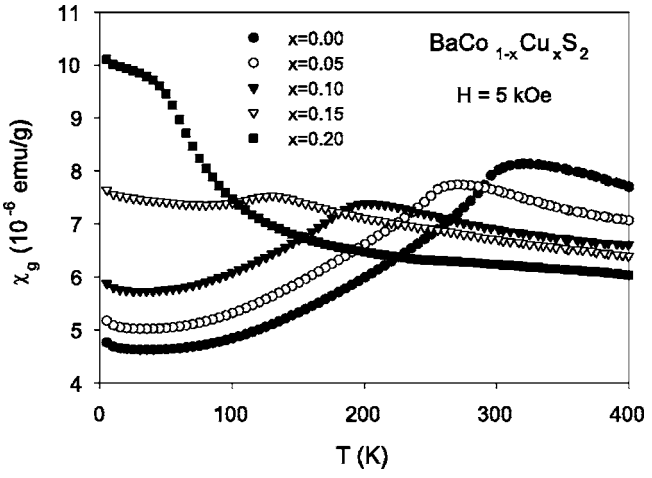

FIG. 3. Magnetic susceptibility as a function of temperature on cooling in a 5 kOe field for Cu content $x \leqslant 0.2$.

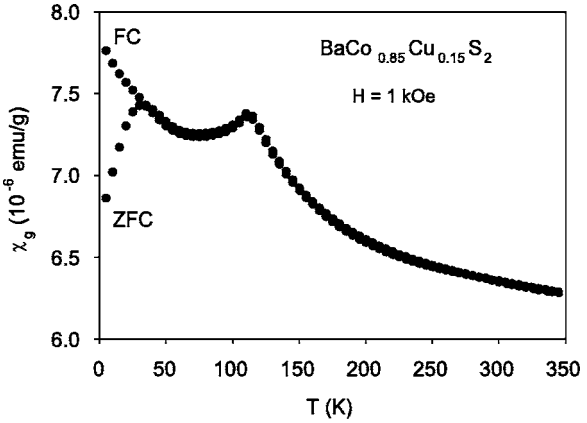

FIG. 4. ZFC and FC magnetic susceptibilities as a function of temperature using a 1 kOe field.

At low temperatures there is evidence for a spin-glass phase in all the Cu-doped compounds. Figure 4 shows the magnetic susceptibility of a $BaCo_{0.85}Cu_{0.15}S_2$ sample obtained in a zero-field-cooled/field-cooled (ZFC/FC) set of measurements. The sample was first cooled to 5 K in zero magnetic field, a 1 kOe field was applied, and measurements were made on warming from 5 to 350 K and on cooling back to 5 K in the same applied field. In addition to the peak near 110 K associated with the antiferromagnetic transition, there is a splitting of the ZFC and FC data below 30 K. At about the same temperature as the onset of this irreversibility there is a well defined peak in the ZFC susceptibility. The Cu-substituted compounds in the paramagnetic region $(x > 0.2)$ as well as those in the antiferromagnetic region $(x < 0.2)$ exhibit similar irreversibility in the ZFC/FC magnetization and a peak in the ZFC data. The peak temperature depends on the Cu content x, and has a maximum value of about 45 K near $x = 0.2$.

This peak in the ZFC susceptibility broadens and shifts to lower temperatures with increasing field as can be seen in Fig. 5 where the ZFC/FC susceptibilities at several different applied fields are shown for a $BaCo_{0.75}Cu_{0.25}S_2$ sample at temperatures in the vicinity of the peak. Also below the irreversibility temperature the susceptibilities exhibit long-time relaxation effects. The ZFC/FC irreversibility, the field-dependent ZFC peak, and the time dependences are all consistent with spin-glass behavior with a freezing temperature $T_f(x)$ defined by the onset of the ZFC/FC irreversibility.

D. ac magnetic susceptibility

ac susceptibility measurements at frequencies between 0.1 and 1000 Hz were made as a function of temperature near T_f on compounds of several different Cu compositions in order to further characterize the low temperature magnetic phase. Results were obtained for the in-phase or real part $\chi'(\omega, T)$ and the out-of-phase or imaginary part $\chi''(\omega, T)$ of the complex susceptibility. The $\chi'(\omega, T)$ obtained for a $BaCo_{0.5}Cu_{0.5}S_2$ sample is shown in Fig. 6.

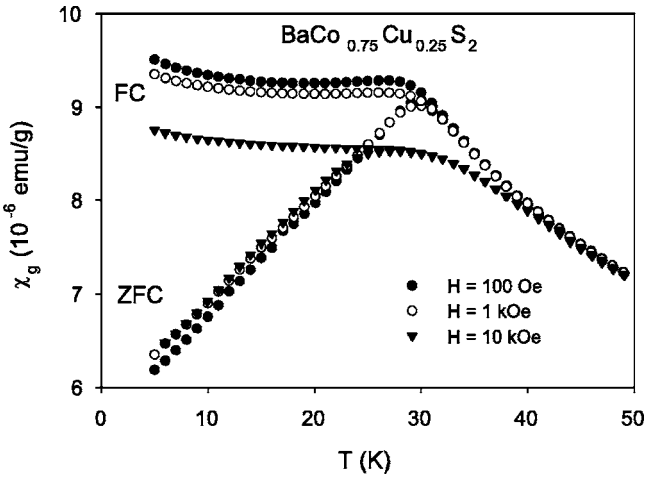

FIG. 5. Field dependence of the ZFC and FC susceptibilities near the freezing temperature.

The temperature at which the maximum of χ' occurs increases with increasing frequency as typical for a spin glass. The value of the relative frequency shift of the maximum in χ' per decade change in frequency, $\Delta T_f/[T_f \Delta(\log \omega)]$, is approximately 0.02. The observed 2% for this parameter is about twice typical for dilute metallic spin glasses and several times smaller than typical for insulating spin glasses.[16]

On the low temperature side of the peak χ' shows a frequency dependence that is approximately logarithmic over this frequency range, while on the high temperature side χ' becomes frequency independent and shows a Curie $1/T$ temperature dependence. The imaginary component χ'', not shown, is nearly frequency independent and about two orders of magnitude smaller than the real component on the low temperature side, and rapidly approaches zero on the high temperature side of the peak. At the lower frequencies χ'' is in excellent agreement with $\chi'' \approx (\pi/2)\partial\chi'/\partial \ln \omega$, which is typical for spin glasses. At higher frequencies the imaginary component becomes so noisy that reproducible measurements could not be made at frequencies above 100 Hz.

This canonical spin-glass behavior is exhibited by all the samples. The freezing temperature T_f depends on the Cu

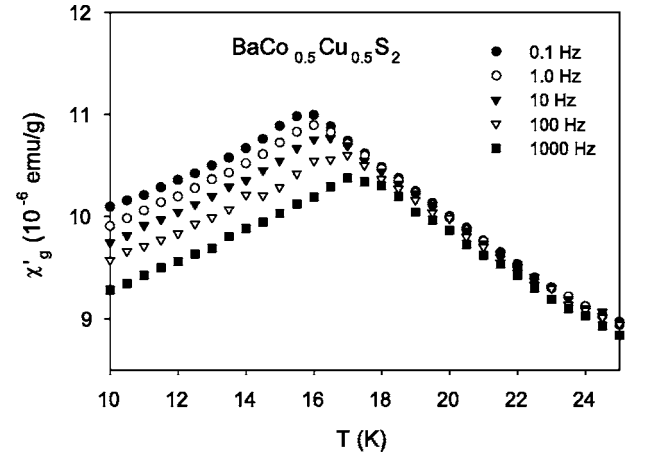

FIG. 6. Frequency dependence of the real part of the ac magnetic susceptibility near the freezing temperature.

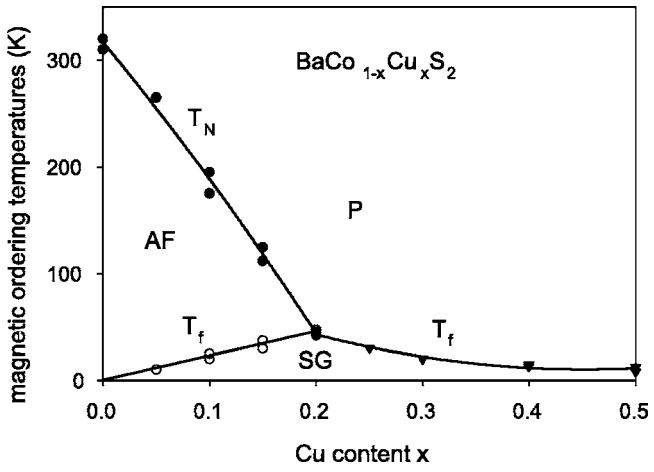

FIG. 7. Magnetic phase diagram (temperature vs composition) showing the antiferromagnetic (AF), paramagnetic (P), and spin-glass (SG) regions constructed from the susceptibility measurements.

content x, decreasing from a maximum of 45 K near $x=0.2$ to zero as x goes to zero and to about 15 K at $x=0.5$. For samples having $x<0.2$, where the transition at T_f is within an antiferromagnetic phase, the behavior of $\chi(\omega,T)$ is similar to that for the $x>0.2$ samples where the freezing is from a paramagnetic phase. In both cases the frequency dependence of $\chi'(\omega,T)$ is logarithmic on the low temperature side of the peak, and at the lower frequencies $\chi'' \approx (\pi/2)\partial\chi'/\partial \ln \omega$. Similarly the peak in χ' shifts to higher temperatures with increasing frequencies, however the parameter $\Delta T_f/[T_f \Delta(\log \omega)]$ is only about half as large in the $x<0.2$ materials.

IV. DISCUSSION

The $BaCo_{1-x}Cu_xS_2$ magnetic phase diagram derived from the measurements is shown in Fig. 7. The lines are estimates for the phase boundaries based on the Néel temperatures $T_N(x)$ and the freezing temperatures $T_f(x)$ that were determined by the positions of the peaks in the susceptibilities. The label P denotes the paramagnetic phase, AF the antiferromagnetic phase, and SG the spin glass phase. The compounds are semiconducting over the entire range of Cu compositions for which compounds could be prepared, namely $x \leqslant 0.5$. The Néel temperature $T_N(x)$ decreases rapidly with x apparently reaching zero by $x \approx 0.2$. The freezing temperature $T_f(x)$ appears discontinuous near $x=0.2$, and can be described by $T_f(x)=(225\ \mathrm{K})\cdot x$ in the $x \leqslant 0.2$ region. In the $x \geqslant 0.2$ region there is an initial rapid decrease followed by little or no change for $x \geqslant 0.3$.

In $BaCoS_2$ one pictures neutral $(CoS_{4/4})_2$ sheets with Co^{2+} and S^{2-} ions and localized electrons owing to the existence of a Mott-Hubbard gap. Since the normal valency of Cu is +1 in chalcogenides, it is surprising that Cu can be substituted for Co more than dilutely. If the electronic states are localized and the Cu is the diamagnetic Cu^{1+}, it is reasonable to assume that Cu substitution produces a compensating concentration of Co^{3+} states. This picture is somewhat supported

by the fact that one is unable to prepare compounds in this series with $x>0.5$. However, if the electronic states are extended, the Co would be uniformly oxidized to a value near $+(2+x)$ depending on the covalent mixing of the Co and S states. The fact that the susceptibilities exhibit Curie-Weiss behavior at high temperatures and that the resistivities decrease with increasing temperatures would seem to favor the localized picture over one where there are partially filled bands with itinerant electrons.

In the case of purely localized states, the Co $3d_{x^2-y^2}$ orbital is likely to be empty owing to the typically large splitting associated with the square pyramidal coordination. This would result in the low-spin configuration where Co^{2+} has $S=1/2$ and Co^{3+} has $S=0$. However, the Co ions will have the high-spin states with $S=3/2$ and 2 for Co^{2+} and Co^{3+}, respectively if the Coulomb interaction leading to Hund's first rule is sufficiently large. Existing high-temperature (350–800 K) magnetic susceptibility data[17] are consistent with Co^{2+} in $BaCoS_2$ having the low-spin configuration. It was shown that this high-temperature data could be well described by Curie-Weiss behavior, $\chi(T)=\chi_0+C/(T+\theta)$ with $\chi_0=5.3(1)\times10^{-6}$ emu/g, $C=1.6(1)\times10^{-3}$ emu K/g, and $\theta=80(20)$ K. This value for the Curie constant C gives a μ_{eff} per Co atom equal to 1.83 μ_B which corresponds to a spin $S=1/2$ with a reasonable $g=2.1$. Also high-temperature (500–770 K) susceptibility data[18] for $Ba_{1-x}Bi_xCoS_2$ ($0\leqslant x\leqslant0.07$) has been fit to yield $\mu_{eff}=1.85$ μ_B/Co. However, refinements of neutron powder diffraction data[6,14,15] for the low-temperature antiferromagnetic phase yield values near 3 μ_B for the ordered Co moment. This appears to be more consistent with the $S=3/2$ high-spin configuration. Also theoretical arguments[19] generally favor the high-spin configuration. Unfortunately there has been no explanation for these apparently contradictory results for the spin configuration of Co^{2+} in $BaCoS_2$. Adding to the confusion are neutron powder diffraction data[6,14,20] for $BaCo_{1-x}Ni_xS_2$ with $0.1\leqslant x\leqslant0.2$ that give ordered Co moments near 1.8 μ_B.

The $BaCo_{1-x}Cu_xS_2$ magnetic susceptibility data for high temperatures (above T_N or T_f) were fit to $\chi(T)=\chi_0+C/(T+\theta)$. The results for the Curie constant C and the temperature independent χ_0 as a function of Cu content x are shown in Fig. 8. Except for $x=0$, the susceptibilities could be well described with the Weiss constant θ set equal to zero. If the Curie-law behavior seen in the $BaCo_{1-x}Cu_xS_2$ series originated from a mixture of independent Co^{2+} and Co^{3+} ions in the ratio $1-x$ to x, the Curie constant for $x\leqslant0.5$ should be proportional to $(1-2x)$ for low-spin or $\left(1-\frac{2}{5}x\right)$ for high-spin. Clearly the manner that the Curie constant C varies with Cu concentration x rules out any description of the Cu doped compounds in terms of independent paramagnetic Co ions. The value of χ_0 does not depend strongly on the concentration of Cu, but does exhibit a nonmonotonic dependence that correlates with the nonmonotonic dependence seen in the resistivity. This positive temperature independent contribution is an order of magnitude larger than the Pauli paramagnetic susceptibility of the metallic $BaNiS_2$ compound.[3,4,8] The large χ_0 suggests that there are near excited states that give rise to a large Van Vleck orbital paramagnetic contribution.

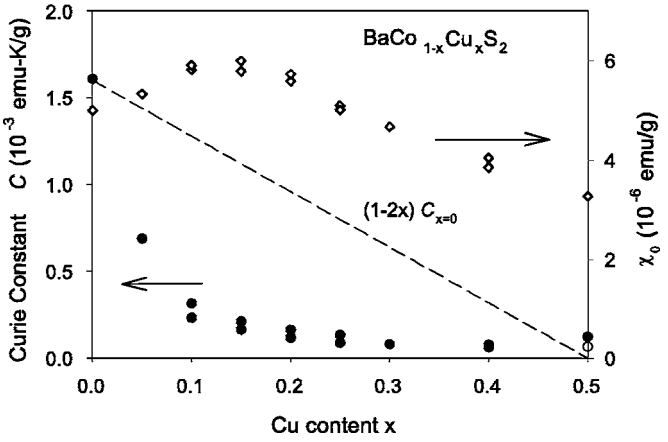

FIG. 8. Dependence of Curie constant C and temperature-independent χ_0 on the Cu content x.

The static and dynamic behavior found in the region identified as a spin-glass phase is fully consistent with a typical spin glass. The ZFC/FC irreversibility, the field-dependent ZFC peak, and the characteristic frequency dependence of the ac susceptibility provide clear evidence for this identification. The small value of the Curie constant shows that the moments freezing at the spin-glass transition are not the spins of individual Co^{2+} ions. Although the Curie contribution is small, it is almost certainly intrinsic to these compounds. The Curie law contribution to these materials from impurities can be estimated from the low temperature paramagnetic tail seen in $BaCoS_2$ which yields a Curie constant about two orders of magnitude smaller then that found for $BaCo_{0.5}Cu_{0.5}S_2$.

It is interesting to compare the behavior seen in the $BaCo_{1-x}Cu_xS_2$ series with several related systems. We have investigated the stoichiometric compounds $Ba_{1-x}La_xCo_{1-x}Cu_xS_2$, where normal valences occur. In this system the magnetic properties are consistent with a localized description with independent $S=1/2$ Co^{2+} and $S=0$ Cu^{1+} ions. Figure 9 shows susceptibility and resistivity data for a $Ba_{0.5}La_{0.5}Co_{0.5}Cu_{0.5}S_2$ sample together with data for $BaCoS_2$ and $BaCo_{0.5}Cu_{0.5}S_2$ for comparison. The susceptibility of the paramagnetic insulator $Ba_{0.5}La_{0.5}Co_{0.5}Cu_{0.5}S_2$ is well described by the Curie-Weiss law over the entire temperature range of the measurement. The fit to the data shown by the solid line in Fig. 9(a) yields $C=8.15\times10^{-4}$ emu K/g, $\chi_0=6.02\times10^{-7}$ emu/g, and $\theta=20$ K. The Curie constant is approximately half that for $BaCoS_2$, and corresponds to a μ_{eff}/Co=1.84 μ_B as expected for independent Co^{2+} ions with $S=1/2$. The value of χ_0 is about an order of magnitude smaller than for $BaCoS_2$ and $BaCo_{0.5}Cu_{0.5}S_2$. In Fig. 9(b) the resistivity for temperatures above 50 K is plotted on a logarithmic scale as a function of $1/T$. The resistivity of $Ba_{0.5}La_{0.5}Co_{0.5}Cu_{0.5}S_2$ is several orders of magnitude greater than that of $BaCoS_2$, and does not exhibit the rapid saturation at lower temperatures. If one fits the resistivities at the highest temperatures to $\rho(T)\propto\exp(E_a/kT)$ the value of E_a is similar for both compounds. However, the resistivity of $Ba_{0.5}La_{0.5}Co_{0.5}Cu_{0.5}S_2$ is quite well described by $\rho(T)\propto\exp[(T_0/T)^{1/2}]$ as shown by the

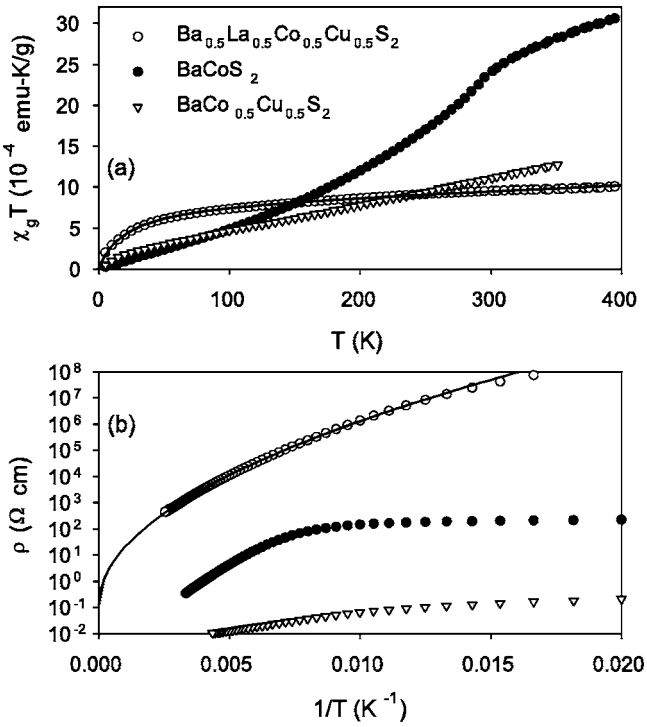

FIG. 9. (a) Susceptibility times temperature vs temperature and (b) resistivity vs inverse temperature for $Ba_{0.5}La_{0.5}Co_{0.5}Cu_{0.5}S_2$ and related compounds.

solid line that is the fit of this expression to the data with $T_0=2.64\times10^4$ K. This behavior is indicative of variable range hopping where there is a Coulomb gap as expected for these compounds.

In the case of the $BaCo_{1-x}Ni_xS_2$ series[3,4,8] substitution of Ni on Co sites produces a continuous change from the antiferromagnetic semiconducting phase to a paramagnetic metallic phase with the crossover in both the electrical and magnetic properties occurring near $x=0.25$. Recently high-resolution angle-resolved photoemission spectroscopy[21] (ARPES) has been used to clarify the electronic structure and the importance of strong electron correlations on both sides of this metal-insulator transition. Results are consistent with a finite Mott-Hubbard energy gap in the insulating phase and a Fermi energy in the metallic phase that crosses a Hubbard band that originates predominantly from the $3d_{z^2-r^2}$ orbital. There appears to be a continuous evolution of the electronic structure where electron correlation becomes less important as the Ni content increases such that band calculations[22,23] can adequately describe the metallic $BaNiS_2$ compound. In this series the initial decrease in T_N with x is about a factor of 4 slower than for the Cu substitution and there is no spin glass phase at low temperature. In this Ni substituted series the μ_{eff} per Co atom derived from the Curie-Weiss behavior above T_N is much smaller than would arise from independent $S=1/2$ Co^{2+} and $S=0$ Ni^{2+} ions as might be expected near a crossover to a metallic phase.

However, in contrast to Ni in $BaCo_{1-x}Ni_xS_2$, Cu in $BaCo_{1-x}Cu_xS_2$ should be a hole dopant. If the holes were localized at sites occupied by Co atoms, one would have the mixture of Co^{2+} and Co^{3+} that is ruled out by the susceptibility results unless clusters of antiferromagnetically correlated spins exist above the ordering temperature. If the holes are itinerant, one would expect a crossover to metallic behavior in the $(Co_{1-x}Cu_xS_{4/4})_2$ sheets as x increases to a significant fraction, but this is not seen in the resistivity results. Neither simple picture can describe the observations. It is clear that strong electron correlation and strong disorder play essential roles in characterizing the electronic states of the $BaCo_{1-x}Cu_xS_2$ compounds.

In addition to the problem of the understanding how the electronic structure changes with the Cu substitution, there is the problem of understanding the spin-glass behavior. The magnetic phase diagram of Fig. 7 is remarkably similar to that of $La_{2-x}Sr_xCuO_4$ for $x<0.06$. This well-studied system,[24] belonging to the simplest structure class of the high-T_C cuprate superconductors, has a zero-temperature insulator to superconductor transition with increasing x at $x=0.06$. The Néel temperatures and spin-glass ordering temperatures of $La_{2-x}Sr_xCuO_4$ as a function of Sr content from a compendium of literature data are shown in Figs. 10.3 and 10.4, respectively of Ref. 24. In their insulating regimes both $La_{2-x}Sr_xCuO_4$ and $BaCo_{1-x}Cu_xS_2$ exhibit a phase with long-range three-dimensional antiferromagnetic ordering with an in-layer arrangement of the moments and also canonical spin-glass behavior at low temperatures. In $La_{2-x}Sr_xCuO_4$ the antiferromagnetic region extends to near $x=0.02$, and at low temperatures there is a spin-glass phase that coexists with the long-range antiferromagnetic order. Here the magnetic entity that freezes is believed to be a spin distortion in the CuO_2 plane bordering each Sr ion. For $0.02<x<0.06$, there is a low-temperature spin-glass phase where the Curie constant for the susceptibility above the spin-glass transition is anomalously small. This spin-glass phase is identified as a cluster spin glass, and a microscopic model for the spin texture has been created[25] to quantitatively explain this anomalously small Curie constant.

The short-range two-dimensional antiferromagnetic correlations that are required for the description of the spin-glass phases in $La_{2-x}Sr_xCuO_4$ are clearly shared by $BaCo_{1-x}Cu_xS_2$. Therefore, it is reasonable to assume that the spin-glass phase in $BaCo_{1-x}Cu_xS_2$ for $x<0.2$ coexists with the antiferromagnetic order and is associated with a magnetic distortion located in the neighboring Co sites at each Cu site. It is interesting to note that the phase diagram for both systems show that $T_f(x)$ depends linearly on x in this region. For $x>0.2$, the much smaller Curie constant C than predicted for independent paramagnetic Co ions indicates that the spin-glass phase in this region is formed out of clusters of antiferromagnetically correlated spins. However, this is only a very general picture without any microscopic details for the moments involved.

The compounds La_2CuO_4 and $BaCoS_2$ have nearly identical antiferromagnetic structures if Co^{2+} is low spin $S=1/2$, and also their Néel temperatures are about the same indicating that the strength of the exchange coupling of the moments is very similar in both systems. However, the electronic structures of these compounds are likely to be significantly different owing to the very different chemical environment of the transition metal ion. Although both are layered compounds, Cu is octahedrally coordinated in

La_2CuO_4 and these octahedrons vertex share to form the CuO_2 layers, while Co in $BaCoS_2$ is in the lower symmetry square pyramidal coordination and these pyramids edge share to form the Co_2S_2 layers. Owing to the importance of strong electron correlation, simple band calculations cannot reliably describe the electronic structures. The recent ARPES study[21] of $BaCo_{1-x}Ni_xS_2$ near the metal-insulator transition identifies some of the differences. In addition, the doping involved in the $La_{2-x}Sr_xCuO_4$ and $BaCo_{1-x}Cu_xS_2$ systems is very different. The Cu doping of $BaCoS_2$ is expected to introduce holes in the Co_2S_2 layers but it also introduces disorder in these layers, while the Sr doping of La_2CuO_4 only introduces holes that reside principally in the CuO_2 layers. Therefore disorder is expected to be very important in the $BaCo_{1-x}Cu_xS_2$ system. Also the level of doping required for a particular magnetic phase is an order of magnitude larger in the $BaCo_{1-x}Cu_xS_2$ system. Thus it seems that understanding the $BaCo_{1-x}Cu_xS_2$ system will involve considerable new physics, however, the remarkable similarities with the normal state $La_{2-x}Sr_xCuO_4$ suggest that further studies of $BaCo_{1-x}Cu_xS_2$ that elucidate microscopic properties would have potential for contributing to our understanding of the cuprate superconductors.

*Electronic address: john-schweitzer@uiowa.edu

[1] F. J. DiSalvo, *Chemistry of High-Temperature Superconductors*, edited by D. L. Nelson, M. S. Whittingham, and T. F. George (American Chemical Society, Washington, DC, 1987), p. 49.
[2] G. J. Snyder, M. C. Gelabert, and F. J. DiSalvo, J. Solid State Chem. **113**, 355 (1994).
[3] L. S. Martinson, J. W. Schweitzer, and N. C. Baenziger, Phys. Rev. Lett. **71**, 125 (1993).
[4] J. Takeda, K. Kodama, H. Harashina, and M. Sato, J. Phys. Soc. Jpn. **63**, 3564 (1994).
[5] J. Takeda, Y. Kobayashi, K. Kodama, H. Harashina, and M. Sato, J. Phys. Soc. Jpn. **64**, 2550 (1995).
[6] K. Kodama, S. Shamoto, H. Harashina, J. Takeda, M. Sato, K. Kakurai, and M. Nishi, J. Phys. Soc. Jpn. **65**, 1782 (1996).
[7] Y. Yasui, Y. Kobayashi, J. Takeda, S. Shamoto, and M. Sato, J. Phys. Soc. Jpn. **65**, 2757 (1996).
[8] L. S. Martinson, J. W. Schweitzer, and N. C. Baenziger, Phys. Rev. B **54**, 11265 (1996).
[9] C. Looney, J. S. Schilling, L. S. Martinson, and J. W. Schweitzer, Phys. Rev. Lett. **76**, 4789 (1996).
[10] J. W. Schweitzer, L. S. Martinson, N. C. Baenziger, D. C. Swenson, V. G. Young, Jr., and I. Guzei, Phys. Rev. B **62**, 12792 (2000).
[11] W. J. Zhu, S. T. Ting, H. H. Feng, and P. H. Hor, J. Solid State Chem. **138**, 111 (1998).
[12] I. E. Grey and H. Steinfink, J. Am. Chem. Soc. **92**, 5093 (1970); J. T. Maynard, E. I. du Pont de Nemours and Company, U.S. Patent No. 2,770,528 (Nov. 1956).
[13] N. C. Baenziger, L. Grout, L. S. Martinson, and J. W. Schweitzer, Acta Crystallogr., Sect. C: Cryst. Struct. Commun. **C50**, 1375 (1994).
[14] S. Shamoto, K. Kodama, H. Harashina, M. Sato, and K. Kakurai, J. Phys. Soc. Jpn. **66**, 1138 (1997).
[15] D. Mandrus, J. L. Sarrao, B. C. Chakoumakos, J. A. Fernandez-Baca, S. E. Nagler, and B. C. Sales, J. Appl. Phys. **81**, 4620 (1997).
[16] See Table 3.1 in J. A. Mydosh, *Spin Glasses: An Experimental Introduction* (Taylor & Francis, London, 1993), p. 67.
[17] M. C. Gelabert, R. J. Lachicotte, and F. J. DiSalvo, Chem. Mater. **10**, 613 (1998).
[18] A. Irizawa, K. Yoshimura, K. Kosuge, C. Dusek, H. Michor, and G. Hilscher, J. Phys. Soc. Jpn. **68**, 3016 (1999).
[19] J.-S. Zhou, W. J. Zhu, and J. B. Goodenough, Phys. Rev. B **64**, 140101(R) (2001).
[20] S. A. M. Mentink, T. E. Mason, B. Fisher, J. Genossar, L. Patlagan, A. Kanigel, M. D. Lumsden, and B. D. Gaulin, Phys. Rev. B **55**, 12375 (1997).
[21] T. Sato, H. Kumigashira, D. Ionel, T. Takahashi, I. Hase, H. Ding, J. C. Campuzano, and S. Shamoto, Phys. Rev. B **64**, 075103 (2001).
[22] L. F. Mattheiss, Solid State Commun. **93**, 879 (1995).
[23] I. Hase, N. Shirakawa, and Y. Nishihara, J. Phys. Soc. Jpn. **64**, 2533 (1995).
[24] For a comprehensive review of experimental results see D. C. Johnson, *Handbook of Magnetic Materials*, edited by K. H. J. Buschow (North-Holland, Amsterdam, 1997) Vol. 10, p. 1.
[25] R. J. Gooding, N. M. Salem, R. J. Birgeneau, and F. C. Chou, Phys. Rev. B **55**, 6360 (1997).